Catalysis Today 147 (2009) 94–99

Contents lists available at ScienceDirect

Catalysis Today

journal homepage: www.elsevier.com/locate/cattod

Hydrotalcite derived Cu-Zn-Cr catalysts admixed with γ-Al_2O_3 for single step dimethyl ether synthesis from syngas: Influence of hydrothermal treatment

Akula Venugopal [a,*], Jelliarko Palgunadi [b], Jung-Kwang Deog [b,**], Oh-Shim Joo [b], Chae-Ho Shin [c]

[a] Catalysis & Physical Chemistry, Indian Institute of Chemical Technology, Tarnaka, Hyderabad 500607, India
[b] Hydrogen Energy Research Center, Korea Institute of Science and Technology, Cheongryang P.O. Box 131, Seoul, Republic of Korea
[c] Department of Chemical Engineering, Chungbuk National University, Cheongju, Chungbuk 361-763, Republic of Korea

ARTICLE INFO

Article history:
Available online 7 April 2009

Keywords:
Cu-Zn-Cr
Hydrotalcite
Dimethyl ether
Syngas conversion
ESR
N_2O decomposition

ABSTRACT

The Cu-Zn-Cr catalysts derived from hydrotalcite (HT) structures were prepared by the hydrothermal and non-hydrothermal methods. The catalysts were admixed with Al_2O_3 to synthesize DME (dimethyl ether) from syngas. XRD analysis revealed the presence of hydrotalcite (HT)-like structures in the oven dried form was decomposed to disperse copper species in the calcined conditions. ESR spectra of the fresh calcined catalysts disclosed both the isolated and clustered copper species and bulk Cr^{3+} species are seen in used catalysts. The TPR analysis indicated that the Cu^{2+} ions are reduced in two stages. DME synthesis experiments showed that the CO conversion and DME yield were linearly correlated with Cu metal surface areas of Cu-Zn-Cr catalysts admixed with γ-Al_2O_3. Activity results indicated that hydrothermal treatments have pronounced influence on the dispersion of copper species and consequently on DME synthesis rates.

1. Introduction

The syngas conversion to dimethyl ether (DME) has been a topic of interest in recent times due to growing demand to replace petroleum based fuel. DME can be produced on the admixed catalysts with the Cu-Zn-Cr for methanol synthesis and solid acid catalysts for methanol dehydration in a single step. It indicates that DME synthesis rates can be controlled by the ratio of methanol synthesis/methanol dehydration activity. The precursors of Cu-Zn-Cr hydrotalcite-like (HTlc) structures generate small clusters of Cu, the active species for the conversion of syngas to methanol. However, it was shown that DME synthesis rate could be determined by the activity of methanol synthesis catalysts on the admixed catalysts with γ-Al_2O_3 [1].

During the DME synthesis three consecutive reactions are possible namely methanol synthesis, methanol dehydration and water gas shift reaction.

$CO + 2H_2 \leftrightarrow CH_3OH$ methanol synthesis

$2CH_3OH \leftrightarrow CH_3OCH_3 + H_2O$ methanol dehydration

$CO + H_2O \leftrightarrow CO_2 + H_2$ water gas shift reaction

Cu based catalysts can control the reaction rates of both methanol synthesis and water gas shift reaction. The copper particle size and dispersion is dependent upon the preparation conditions such as Cu/Zn mole ratio, precipitation pH and heat treatments during and after the precipitation [2–4]. The conversion of syngas to methanol is dependent upon the copper metal surface area and finely dispersed copper can be obtained through the precursors of ternary Cu-Zn-Cr hydrotalcite structures prepared by a co-precipitation method and subsequent thermal decomposition [5,6].

Introduction of small amounts of trivalent metal ions into Cu–ZnO matrix enables the formation of cationic defects in catalyst structure and these cationic defects enrich and stabilize copper on the surface of Cu based catalysts for methanol synthesis during reduction and reaction [7]. In the present study we attempted to synthesize the Cu-Zn-Cr hydrotalcite precursors with and without thermal treatment during preparation in order to study the role of metal cation with respect to copper metal surface area and CO conversions.

The Cu-Zn-Cr with and without thermal treatment catalysts were characterized by BET surface area, powder XRD, TPR, SEM–EDX, and ESR analyses, and the syngas conversions on the admixed catalysts of Cu-Zn-Cr with γ-Al_2O_3 were measured under the conditions of 240–280 °C and 600 psig. The Cu surface areas were measured by N_2O titration method to correlate the DME activity with the Cu surface areas of Cu-Zn-Cr catalysts.

* Corresponding author. Tel.: +91 40 27193510; fax: +91 40 27160921.
** Corresponding author. Tel.: +82 2 958 5218; fax: +82 2 958 5219.
E-mail addresses: akula@iict.res.in (A. Venugopal), jkdcat@kist.re.kr (J.-K. Deog).

0920-5861/$ – see front matter © 2009 Elsevier B.V. All rights reserved.
doi:10.1016/j.cattod.2009.03.003

2. Experimental

2.1. Catalyst preparation

Catalyst precursors were prepared by the co-precipitation method with mol% ratios of Cu:Zn:Cr = 44:44:12 and Cu:Zn:Cr = 47:38:15 with and without hydrothermal treatment during the preparation. About 0.6 L aqueous solution of copper, zinc, chromium nitrates (solution A) and a solution B containing 2 M NaOH and 1 M Na_2CO_3 (1:1 = v/v) were added simultaneously to 2.0 L of distilled water under vigorous stirring. The rate of addition of solution A was approximately 0.5 L/h while maintaining a constant pH ~8.0 ± 0.1 by adjusting the flows of solutions A and B. The co-precipitation is carried out at room temperature and subsequently the precipitate was separated in to two portions. One portion of the precipitate was (Gel A: without hydrothermal treatment) washed and filtered and the other portion of the precipitate was kept at 70 °C for 1 h (Gel B: hydrothermal treated) subsequently washed several times until the pH of the gel reached the pH of the distilled water that has been used for the preparation. The residual Na content is found to be <0.03% measured by atomic absorption spectroscopy in all the precipitates i.e. hydrothermal and non-hydrothermal treated. The precipitates were oven dried at 100 °C for 24 h and calcined in static air at 400 °C for 3 h.

2.2. Characterization

The BET surface areas of the calcined catalysts were obtained by dinitrogen physisorption at −196 °C using a Micromeritics ASAP 2000 instrument. Prior to the measurements the catalysts were degassed at 120 °C for 0.5 h. The X-ray diffraction analysis of the catalyst samples was carried out in the 2θ range from 5° to 90° using a Rigaku Diffractometer employing Ni filtered Cu K_α radiation at 40 kV and 126 mA. The XRD patterns were compared with ICDD data. The N_2O titrations were carried out using a tubular reactor system connected to a thermal conductivity unit. For N_2O titrations Porapak N column was used for the N_2O and N_2 separation and estimations. In a typical experiment about 30–80 mg of catalyst was loaded and reduced in 5% H_2/Ar stream at 250 °C for 1 h and the reactor was purged in a He stream at 250 °C for 0.5 h and cooled down to 90 °C at which the N_2O titrations were carried out. Several replicate experiments were carried out and the Cu metal surface areas were measured so that the N_2O titration takes place in a single pulse. In this investigation a surface copper density of 1.46×10^{19} atoms/m^2 and Cu:O = 2:1 taken into consideration for the copper metal area measurements [8]. The ESR analysis is performed at room temperature using JEOL, JES-FA200 ESR spectrophotometer by X-band equipment with an operating frequency ν = 9.029 GHz. The scanning electron microscopy (SEM) and energy dispersive X-ray (EDX) analysis performed by HITACHI FE-SEM S – 400 microscope at an accelerating voltage 0.5–30 kV.

2.3. Activity measurements

DME synthesis was carried out in a fixed bed micro reactor (O.D.: 3/8″, Length: 30 cm) loaded with 1.0 g of catalyst composed of 0.5 g of activated methanol synthesis catalyst (Cu-Zn-Cr) and 0.5 g of methanol dehydration catalyst i.e. γ-Al_2O_3. Prior to the reaction the catalysts were reduced in a stream of 5% H_2/Ar in a sequential reduction steps as follows: 1st step: treatment at 100 °C/0.5 h, 2nd step: reduction at 180 °C/0.5 h, 3rd step: reduction at 240 °C/2 h, 4th step: reduction at 280 °C/0.5 h. The reaction was conducted under the condition of 1.5 of H_2 to CO ratio, at a GHSV of 6000 h^{-1}, pressure of 600 psig and the reaction temperature ranged from 240 to 280 °C and the pressure was maintained by means of a back pressure regulator and the gas flow rates were controlled by mass flow controllers. The reaction mixture was passed through a purifier in order to eliminate the traces of water, oxygen and iron carbonyl that would deactivate the catalyst. The effluent gas mixture was analyzed by on-line gas chromatograph equipped with thermal conductivity detector using Porapak Q column. The activity data were collected after 6 h of continuous operation. The experimental error in the activity evaluation of the catalysts was found to be ±2% unless otherwise mentioned.

3. Results and discussion

3.1. XRD analysis

The XRD patterns of the oven dried samples reveal the diffraction lines of Cu-Zn-Cr HTlc structure as shown in Fig. 1 [9,10]. The XRD patterns show sharp signals over hydrothermally treated catalysts than the non-hydrothermally treated catalysts. Presence of CuO phase in oven dried samples is attributed to the Jahn–Teller effect due to the deviant behavior of copper when the Cu/Zn ratio >1 is maintained in the ternary Cu-Zn-Cr catalysts [11]. The diffraction lines due to CuO phase is sharper in hydrothermally treated catalysts than the non-hydrothermally treated samples. XRD patterns of the calcined samples are shown in Fig. 2. The HT structure of Cu-Zn-Cr collapsed upon thermal decomposition in air at 400 °C/3 h. Phase due to CuO and its reflections at 2θ = 35.54°, 38.6°, 35.3°, 48.85° and 38.9° and their corresponding "*d*" values of 0.252, 0.232, 0.253, 0.186 and 0.231 nm [ICDD: 80-0076] are observed. The diffraction lines attributed to ZnO [ICDD: 89-1397] phase appeared at 2θ = 36.2°, 31.7°, 34.34°, 56.5° and 62.7° and the corresponding "*d*" values of 0.247, 0.281, 0.26, 0.162 and 0.147 nm are clearly seen. Phases due to CuO and ZnO are predominant and the $ZnCr_2O_4$ phase [ICDD: 22-1107] (appeared at 2θ = 35.7°, 30.3°, 63.1°, 57.4° and 43.4° with the "*d*" values 0.251, 0.294, 0.147, 0.16, 0.208 nm) is minor in intensity. It is also observed that some of the diffraction lines of ZnO and $ZnCr_2O_4$ are superimposed.

3.2. TPR results

The TPR profiles of the calcined CuO-ZnO-Cr_2O_3 catalysts are reported in Fig. 3. It is observed that the copper oxides in CuO–ZnO–Cr_2O_3 samples are reduced in two stages and these peaks are presumably due to dispersed copper oxide and the clustered CuO.

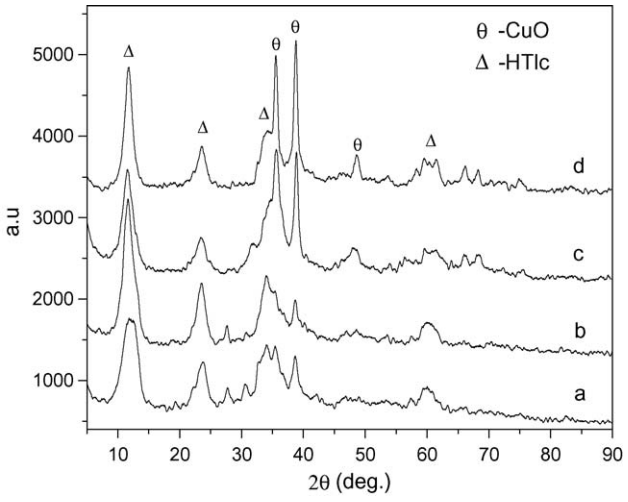

Fig. 1. XRD patterns of the oven dried: (a) Cu:Zn:Cr = 44:44:12 non-hydrothermal treated, (b) Cu:Zn:Cr = 47:38:15 non-hydrothermal treated, (c) Cu:Zn:Cr = 44:44:12 hydrothermal treated and (d) Cu:Zn:Cr = 47:38:15 hydrothermal treated catalysts.

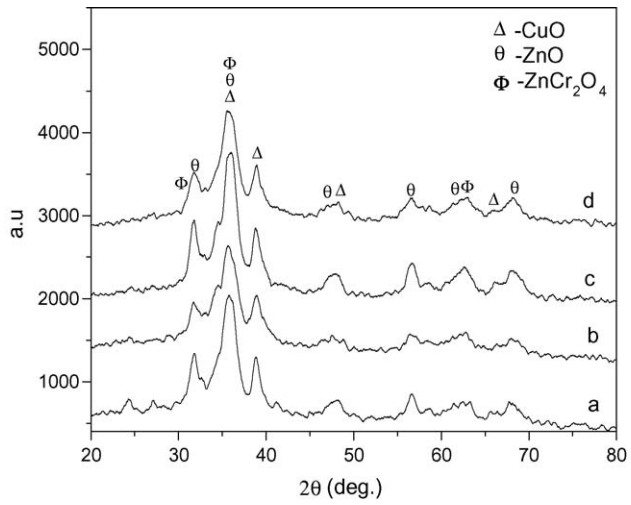

Fig. 2. XRD patterns of the calcined: (a) Cu:Zn:Cr = 44:44:12 non-hydrothermal treated, (b) Cu:Zn:Cr = 44:44:12 hydrothermal treated, (c) Cu:Zn:Cr = 47:38:15 non-hydrothermal treated and (d) Cu:Zn:Cr = 47:38:15 hydrothermal treated catalysts.

The reduction peak is slightly shifted toward high temperatures with hydrothermal treatment indicating that formation of large CuO particles. The non-hydrothermally treated samples are completely reduced below 300 °C. On the other hand hydrothermally treated CuO–ZnO–Cr_2O_3 samples are reduced at slightly higher temperatures. The reduction peak centered at 250 °C is appeared over Cu:Zn:Cr = 44:44:12 catalyst. This reduction peak slightly shifted to higher temperature and emerged at 280 °C upon increase in the copper loading in Cu:Zn:Cr = 47:38:15 catalyst in non-hydrothermally treated catalysts. Where as in case of hydrothermally treated catalysts the first reduction signal is seen at 275 °C with a shoulder peak at 300 °C over Cu:Zn:Cr = 44:44:12 catalyst. A reduction signal due to dispersed copper could be seen at 295 °C with a shoulder peak at 317 °C over Cu:Zn:Cr = 47:38:15 catalyst that under gone hydrothermal treatment. We have earlier observed the similar phenomena during the TPR analysis of CuO-ZnO-Cr_2O_3 catalysts [1]. Finally it is concluded that upon hydrothermal treatment, large size of copper clusters are formed and similar trend is also observed with increase in copper content in the mixed CuO-ZnO-Cr_2O_3 catalysts.

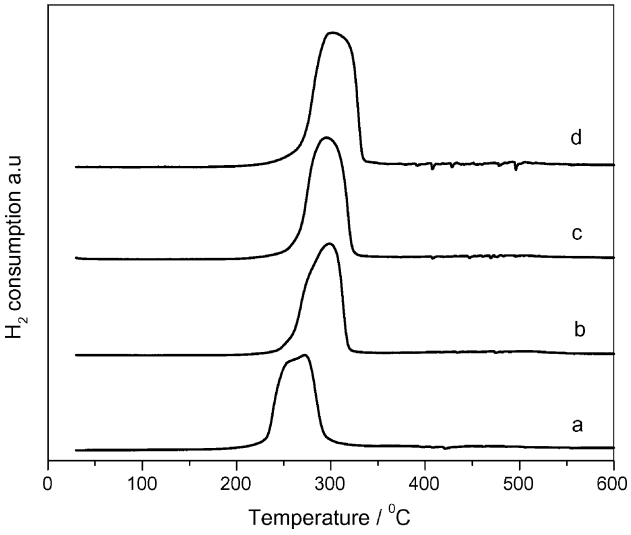

Fig. 3. TPR profiles of the calcined: (a) Cu:Zn:Cr = 44:44:12 non-hydrothermal treated, (b) Cu:Zn:Cr = 44:44:12 hydrothermal treated, (c) Cu:Zn:Cr = 47:38:15 non-hydrothermal treated and (d) Cu:Zn:Cr = 47:38:15 hydrothermal treated catalysts.

3.3. SEM analysis

The SEM pictures of the calcined CuO-ZnO-Cr_2O_3 catalysts are shown in Fig. 4. The elemental compositions of the Cu, Zn, and Cr obtained from the EDX analyses are presented in Table 1. It is observed that the compositions determined by chemical analysis are in close agreement with the nominal compositions taken for the catalysts preparations. The SEM micrographs of the samples Cu:Zn:Cr = 47:38:15 (non-hydrothermally treated Fig. 4a) and Cu:Zn:Cr = 47:38:15 (hydrothermally treated Fig. 4b) reveal that the particles are of uniform shape almost spherical in all the samples but the particles sizes are different. At least 50 particles have been chosen in order to measure the average particle size of the catalysts. Using in situ high resolution TEM investigations, Topsøe [12] and Helveg et al. [13] reported that the Cu-Zn catalysts undergo structural transformation when the catalysts are exposed to syngas mixture. Grunwaldt et al. found that the morphology of copper particles are found to be disk-like shape on the partially reduced ZnO surface, while on the fully oxidized ZnO surface the copper particles became more spherical in shape due to the weak interaction between copper and ZnO [14]. From Fig. 4a and b it is clearly evident that the CuO-ZnO-Cr_2O_3 sample forms larger particles in hydrothermally treated compared non-hydrothermal

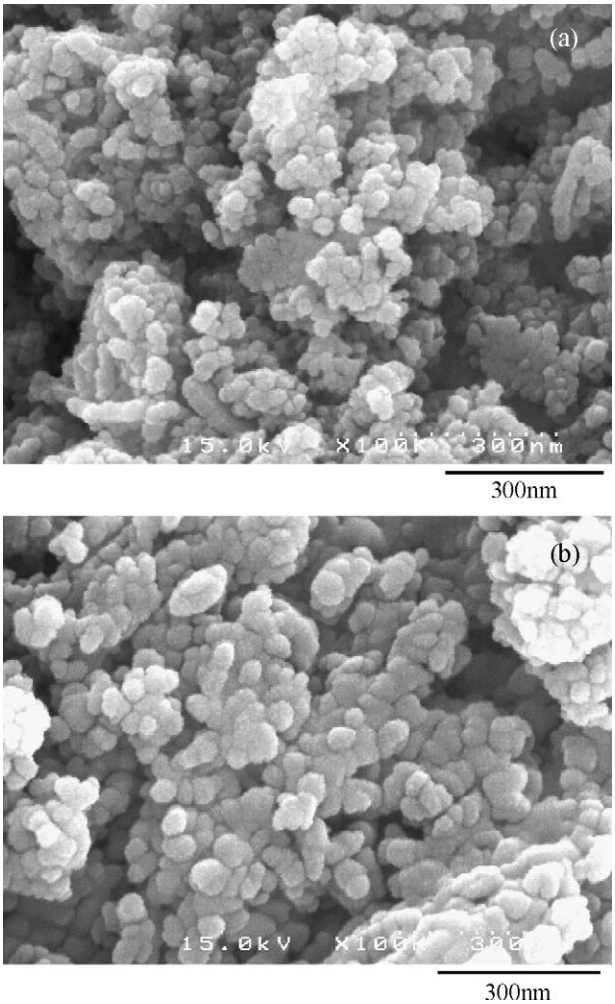

Fig. 4. SEM pictures of (a) Cu:Zn:Cr = 47:38:15 non-hydrothermal treated and (b) Cu:Zn:Cr = 47:38:15 hydrothermal treated catalysts.

Table 1

Nominal Cu:Zn:Cr (mol%)	BET SA (m^2/g)	[a]H_2 uptake (μmol/g)	[b]Actual composition (mol%)	[c]Cu metal surface area (m^2/g)	% CO conversion at 280 °C
44:44:12 A	102.5	299.4	45.2:42.9:11.8	6.6	55.7
44:44:12 B	89.9	323.5	44.2:43.8:11.6	5.3	51.6
47:38:15 A	122.6	350.7	48.9:33.9:17.2	7.2	61.2
47:38:15 B	74.7	525.8	48.6:34.1:17.3	4.9	48.8

A: Catalyst without hydrothermal treatment.
B: Catalyst with hydrothermal treatment at 70 °C.
[a] H_2 uptakes measured from TPR analysis.
[b] From SEM–EDX analysis.
[c] Measured by N_2O decomposition.

treated sample. The average particle size is found to be 64.9 nm in case of hydrothermally treated sample and 43 nm for non-hydrothermal treated catalyst. These results are further supported by the TPR analysis where large particles of CuO were reduced at high temperatures over hydrothermally treated samples and the non-hydrothermal treated CuO underwent the reduction at low temperatures.

3.4. ESR studies

The ESR spectroscopy is used to investigate the paramagnetic species of Cu^{2+}, Cr^{3+} and Cr^{5+} present in the CuO-ZnO-Cr_2O_3 catalysts. The room temperature ESR spectra of the fresh and used catalysts are shown in Fig. 5a and b, respectively. From Fig. 5a it is evident that the peak shapes of the signals attributed to Cu^{2+} and the spectra are anisotropic with clearly defined $g_{||}$ and $g_{\perp}$ regions as expected for Cu^{2+} ions in a surrounding with axial symmetry [1]. The isolated copper species are responsible for the spectrum component with $g_{||} = 2.21$, $A_{||} = 57$ mT a well-resolved hyperfine structure and unresolved hyperfine pattern around $g_{\perp} = 2.09$ is observed. These experimental results are in good agreement with the reported literature [15–17]. Busetto et al. investigated the influence of calcination on the nature of mixed oxides of Cu-Zn-Al formed from a layered double hydroxide system, and observed the occurrence of Cu(II) clustering, albeit at higher temperatures [3]. This suggests that mixed oxides of Cu based catalysts produce copper clusters upon thermal treatment during the course of preparation.

The ESR patterns of the used catalysts are shown in Fig. 5b. Highly symmetrical broad signals, attributed to Cr^{3+} centered at 326.7 mT with corresponding $g = 1.97$ is observed. The ΔH_{pp} is the distance between peaks of the first-order differential quotient and the measured line widths of $\Delta H_{pp} = 69.0$ mT for Cu:Zn:Cr = 44:44:12, $\Delta H_{pp} = 59.6$ mT for Cu:Zn:Cr = 47:38:15 non-hydrothermal treated samples. Where as $\Delta H_{pp} = 71.0$ mT for Cu:Zn:Cr = 44:44:12 and $\Delta H_{pp} = 78.7$ mT for Cu:Zn:Cr = 47:38:15 hydrothermally treated catalysts [18]. The line widths are slightly higher in case of hydrothermal treated samples compared to the non-hydrothermal treated catalysts. The Cr^{3+} species are ascribed due to the presence of $ZnCr_2O_4$ in the catalyst and it is unlikely that these species belong to $CuCr_2O_4$ since XRD patterns of the used catalysts did not show any peaks due to $CuCr_2O_4$ phase. Cu^{2+} signals are absent in used catalysts indicating that all Cu^{2+} species are in the reduced form.

3.5. BET surface areas and N_2O decomposition results

The BET surface areas and the copper metal surface areas of the catalysts are reported in Table 1. It is observed that the hydrothermally treated catalysts have lower BET surface area than the non-hydrothermal treated samples. The copper metal surface areas are slightly higher in case non-hydrothermal treated catalysts compared to the hydrothermal treated catalysts.

3.6. Activity measurements

The syngas conversion to dimethyl ether synthesis over the admixed catalysts composed of Cu-Zn-Cr and the γ-Al_2O_3 catalysts are reported in Fig. 6a–d. It is clearly evident that with increase in reaction temperature, the CO conversions are linearly increased in all the case. A similar tendency is observed with respect to the formation of DME, indicating that CO conversions are linearly related to the DME synthesis rates. Selectivity towards CO_2 is less

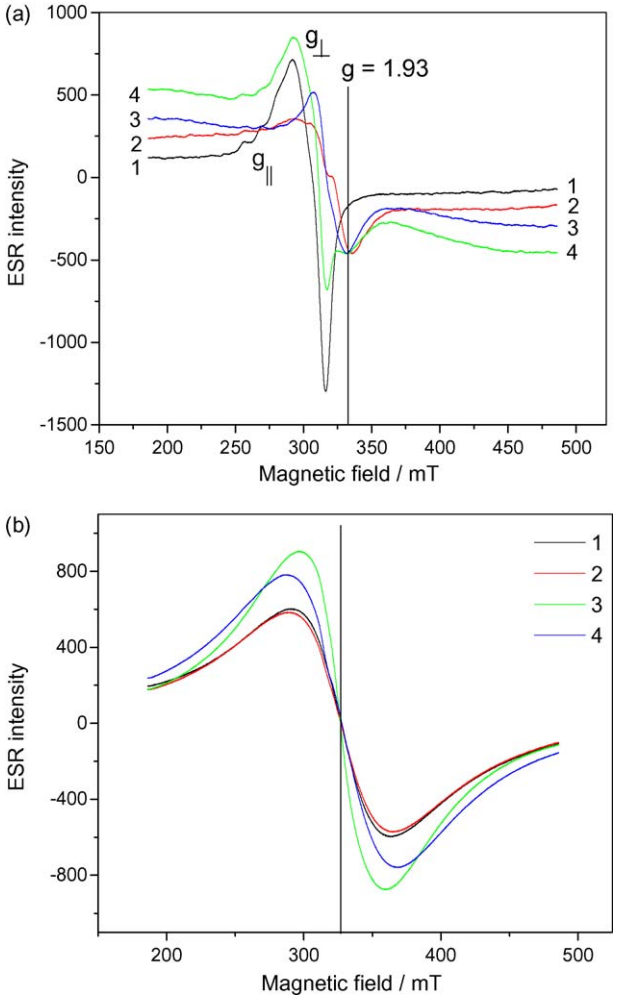

Fig. 5. (a) ESR spectra of the fresh (1) Cu:Zn:Cr = 44:44:12 non-hydrothermal treated, (2) Cu:Zn:Cr = 44:44:12 hydrothermal treated, (3) Cu:Zn:Cr = 47:38:15 hydrothermal treated, (4) Cu:Zn:Cr = 47:38:15 non-hydrothermal treated catalysts. (b) ESR spectra of the used (1) Cu:Zn:Cr = 44:44:12 non-hydrothermal treated, (2) Cu:Zn:Cr = 44:44:12 hydrothermal treated, (3) Cu:Zn:Cr = 47:38:15 non-hydrothermal treated and (4) Cu:Zn:Cr = 47:38:15 hydrothermal treated catalysts.

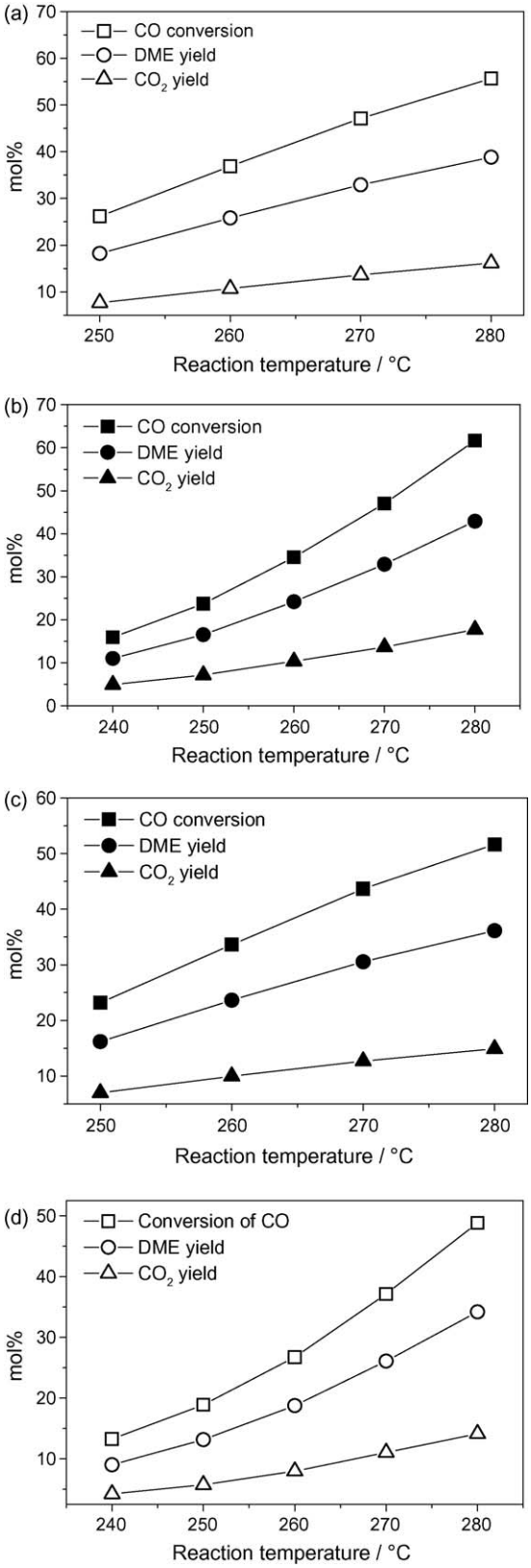

Fig. 6. Syngas conversions, DME and CO_2 yields over, (a) Cu:Zn:Cr = 44:44:12 non-hydrothermal treated, (b) Cu:Zn:Cr = 47:38:15 non-hydrothermal treated, (c) Cu:Zn:Cr = 44:44:12 hydrothermal treated and (d) Cu:Zn:Cr = 47:38:15 hydrothermal treated catalysts. Pressure = 600 psig, H_2/CO = 3/2, GHSV of 6000 h^{-1}.

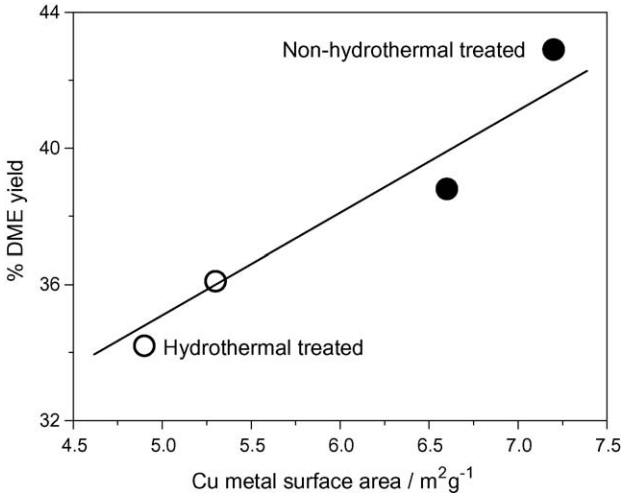

Fig. 7. Copper metal surface area vs. DME yields at a reaction temperature of 280 °C and pressure = 600 psig, H_2/CO = 3/2, GHSV of 6000 h^{-1}.

than 20% over all the catalysts studied. Jun et al have observed the increase in intrinsic activity of Cr_2O_3 promoted CuO-ZnO hybrid catalysts during the CO_2 hydrogenation to produce high DME yields [19,20]. Maximum CO conversion about 61.5% is obtained over a catalyst composition Cu:Zn:Cr = 47:38:15 (mol%) catalyst that is non-hydrothermally treated. The CO conversions are found to be linearly related with the copper metal surface areas (Table 1) measured by N_2O decomposition studies. Fig. 7 represents the relationship between copper metal surface area and DME yields. In the comparative analysis it is clearly visualized that the non-hydrothermally treated catalysts displayed higher DME yields than the hydrothermal treated catalysts.

4. Conclusions

XRD analysis of the oven dried samples revealed the presence of hydrotalcite structure and the finely dispersed copper species in the calcined form. TPR results indicated the two-stage reduction of Cu^{2+} species. Large clusters of particles appeared with uniform shape in SEM analysis with an average particles size of 64.9 nm in case of hydrothermally treated samples. On the contrary non-hydrothermal treated samples pose an average particles size of 43 nm. Presence of both clustered and isolated copper species appeared in ESR analysis of the hydrothermally treated samples. It was observed that the copper metal surface areas of the non-hydrothermally treated samples were higher than that of the hydrothermally treated samples. The syngas conversions over the non hydrothermally treated samples were higher than that over hydrothermally treated samples, which is explained due to the presence of highly dispersed copper species on the catalyst surface. From these studies it can be concluded that the copper species are highly sensitive towards thermal treatments, which could effect the dispersion of copper and consequently on syngas conversions and DME yields.

Acknowledgements

This work is financially supported by a program of Energy and Resources Technology Development. One of the authors AV acknowledges the KOFST, (Korea) for financial support and Director-IICT and CSIR-New Delhi, India.

References

[1] A. Venugopal, J. Palgunadi, K.D. Jung, O.S. Joo, C.H. Shin, Catal. Lett. 123 (2008) 142.
[2] T.H. Fleisch, R.L. Mieville, J. Catal. 90 (1984) 165.

[3] C. Busetto, G.D. Piero, G. Manara, F. Trifiro, A. Vaccari, J. Catal. 85 (1984) 260.
[4] J.M. Campos-Martin, A. Guerrero-Ruiz, J.L.G. Fierro, J. Catal. 156 (1995) 208.
[5] K. Klier, V. Chatikavanij, R.G. Herman, G.W. Simmons, J. Catal. 74 (1982) 343.
[6] J.H. Kim, M. Park, O.S. Joo, K.D. Jung, Appl. Catal. A: Gen. 264 (2004) 37.
[7] J.C. Frost, Nature 334 (1988) 557.
[8] J.W. Evans, M.S. Wainwright, A.J. Bridgewater, D.J. Young, Appl. Catal. 7 (1983) 75.
[9] P. Porta, S. Morpurgo, Appl. Clay Sci. 10 (1995) 31.
[10] S. Morpurgo, M.L. Jacano, P. Porta, J. Solid State Chem. 119 (1995) 246.
[11] F. Trifiro, A. Vaccari, G.D. Piero, in: K.K. Unger, J. Raoquerol, K.S.W. Sing, H. Kral (Eds.), Characterization of Porous Solids, Elsevier, Amsterdam, 1988, p. 571.
[12] H. Topsøe, J. Catal. 216 (2003) 155.
[13] S. Helveg, P.L. Hansen, Catal. Today 111 (2006) 68.
[14] J.-D. Grunwaldt, A.M. Molenbroek, N.-Y. Topsoe, H. Topsoe, B.C. Clausen, J. Catal. 194 (2000) 452.
[15] S. Sakata, T. Nakai, H. Yahiro, M. Shiotani, Appl. Catal. A: Gen. 165 (1997) 467.
[16] T. Tanabe, T. Iijima, A. Koiwai, J. Mijuno, K. Yokota, A. Isogai, Appl. Catal. B: Environ. 6 (1995) 145.
[17] K. Bahranowski, R. Dula, M. Gasior, M. Labanowski, A. Michalik, L.A. Vartikian, E.M. Serwicka, Appl. Clay Sci. 18 (2001) 93.
[18] M. Ralek, W. Gunsser, A. Knappwost, J. Catal. 11 (1968) 317.
[19] K.-W. Jun, M.-H. Jung, K.S. Rama Rao, M.-J. Choi, K.-W. Lee, Stud. Surf. Sci. Catal. 114 (1998) 447.
[20] K.-W. Jun, K.S. Rama Rao, M.-H. Jung, K.-W. Lee, Bull. Korean Chem. Soc. 19 (1998) 466.